Journal of Science and Technology in Civil Engineering, HUCE, 2025, 19 (3): 15–29

SHEAR PERFORMANCE OF PRESTRESSED HOLLOW-CORE SLABS STRENGTHENED WITH CFRP: FINITE ELEMENT MODELING AND PARAMETRIC INSIGHTS

Nguyen Thi Nguyet Hang[a,*], Tran Viet Hung[a], Fan Shengxin[b]

[a]*Faculty of Bridge and Road Engineering, Hanoi University of Civil Engineering, 55 Giai Phong road, Bach Mai ward, Hanoi, Vietnam*

[b]*College of Civil and Transportation Engineering, Guangdong Province Key Laboratory of Durability for Marine Civil Engineering, Key Laboratory on Durability of Civil Engineering in Shenzhen, Shenzhen University, Shenzhen 518060, PR China*

Article history:
Received 28/7/2025, Revised 04/8/2025, Accepted 10/8/2025

Abstract

This study investigates the shear performance of prestressed hollow-core (HC) slabs strengthened with externally bonded carbon fiber-reinforced polymer (CFRP) sheets using finite element modeling (FEM). Three-dimensional FEM models, developed in Abaqus and validated against experimental data, accurately replicate the web-shear failure mode and shear capacity of five full-scale HC slabs under shear-dominated loading, with deviations of less than 5%. A comprehensive parametric study examines the influence of CFRP configuration (bonded length and number of layers), concrete compressive strength, prestressing level, and slab geometry (depth and void shape). The results confirm that CFRP strengthening significantly enhances shear capacity, with optimal performance achieved using two to three layers at a bonded length of 450 mm. Higher concrete strength further amplifies the effectiveness of CFRP, while increased prestressing levels tend to reduce shear capacity due to additional stresses in the web region. Slabs with greater depths and non-circular voids exhibit more pronounced improvements, especially when full-height CFRP strengthening is applied. Comparisons with ACI 318-19 and ACI 440.1R-15 reveal notable discrepancies, emphasizing the limitations of current design provisions and the need for refined analytical approaches. The findings offer practical insights into the design and strengthening of HC slabs and contribute to the development of more accurate and reliable design guidelines.

Keywords: prestressed hollow-core slabs; web-shear failure; shear resistance; FEM; CFRP.

https://doi.org/10.31814/stce.huce2025-19(3)-02 © 2025 Hanoi University of Civil Engineering (HUCE)

1. Introduction

Precast/prestressed concrete hollow-core (HC) slabs are widely used in modern construction due to their structural efficiency, reduced self-weight, and ease of installation [1, 2]. However, the absence of shear reinforcement (stirrups), combined with the presence of longitudinal voids, makes these slabs particularly vulnerable to web-shear failure, a brittle and sudden failure mode that typically initiates in the web and rapidly propagates toward the support or loading region, resulting in diagonal cracks and a sudden loss of load-carrying capacity [3, 4]. This vulnerability is further exacerbated in deeper slabs with non-circular voids, as highlighted in previous research [1, 5–7]. In fact, HC slabs have been shown to fail in web-shear at loads lower than those predicted by existing design codes [1, 8, 9].

Over the past two decades, externally bonded fiber-reinforced polymer (FRP) composites, particularly carbon fiber-reinforced polymer (CFRP), have emerged as an effective technique for enhancing

*Corresponding author. *E-mail address:* hangntn@huce.edu.vn (Hang, N. T. N.)

the shear performance of reinforced and prestressed concrete members, especially those lacking stirrups. Numerous experimental studies have confirmed the potential of CFRP to significantly increase load-bearing capacity and overall performance of concrete structures [10–17]. However, in the context of HC slabs, the unique cross-sectional geometry, characterized by longitudinal voids and thin webs, introduces complex stress distributions and failure mechanisms. Consequently, research on CFRP strengthening of HC slabs remains limited [10, 11, 13, 18].

Among the few available studies, Elgabbas et al. [13] focused on flexural strengthening techniques, while Wu [18] investigated the shear strengthening of single-web prestressed HC slabs using bonded CFRP sheets. Wu's study involved full-scale experimental testing and finite element modeling to evaluate the effectiveness of bonding CFRP along the internal perimeter of slab voids. Key parameters such as CFRP width, length, and number of layers were varied, resulting in notable improvements in both ultimate shear capacity and ductility. However, the study was restricted to single-web configurations and considered only slabs with circular voids.

Subsequently, Meng et al. [10, 11] conducted comprehensive experimental and numerical investigations into the shear strengthening and web-shear behavior of full-sized prestressed HC slabs using externally bonded CFRP sheets. A total of ten full-scale HC units tested under vertical line loads, followed by validated numerical simulations were studied. Key parameters investigated included prestressing level, CFRP sheet length, width, and thickness. Although this work provided valuable insights into the shear behavior of CFRP-strengthened HC slabs, it was limited in scope with respect to the variation of parameters such as CFRP layering and prestressing levels. Moreover, the study focused solely on slabs with circular voids and a depth of 305 mm, leaving the behavior of deeper slabs with non-circular voids largely unexplored.

To address these research gaps, this study presents an extended and comprehensive numerical investigation into the web-shear behavior of HC slabs strengthened with externally bonded CFRP sheets. Validated finite element (FE) models are developed to replicate the response of full-scale slabs under shear-dominated loading conditions. Once verified, the models are used in a series of parametric studies to examine the influence of key variables such as CFRP configuration, concrete compressive strength, prestressing level, and slab geometry. The findings aim to enhance understanding of CFRP strengthening mechanisms in HC slabs and provide valuable guidance for practical design and future code development.

2. Description of investigated slabs

2.1. Details of test specimens

This study utilized five HC slab specimens previously tested by Meng et al. [10] to validate the developed finite element (FE) model and to further investigate the shear resistance of HC slabs strengthened with CFRP. Detailed descriptions of the cross-sections, test setup, and experimental results can be found in Meng et al. [10, 11].

The investigated slabs were 305 mm in height, 1126 mm in width, and had a span length of 4499 mm. They were tested under a three-point bending configuration, as illustrated in Fig. 1. Each slab included four circular voids and was prestressed using eight 13 mm-diameter strands. As reported in the previous studies [10, 11], the slabs were cast using normal-strength concrete with an average 28-day compressive strength of 60 MPa (cylinder strength). The prestressing tendons were 7-wire, low-relaxation strands with a nominal diameter of 13 mm and an ultimate tensile strength of 1860 MPa. All strands were stressed to 67% of their ultimate strength, resulting in an initial prestress of approximately 1246 MPa per strand. To strengthen the slabs, SikaWrap-900C CFRP sheets were applied throughout the entire core, with a bonded length of 450 mm, as shown in Fig. 1(b). The

CFRP sheets had a tensile strength of 1120 MPa and a modulus of elasticity of 100 GPa, as reported in Meng et al. [11].

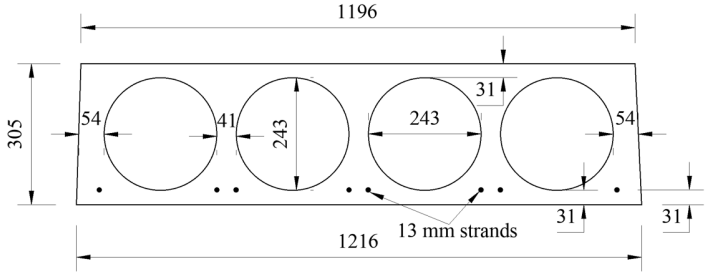

(a) Cross section

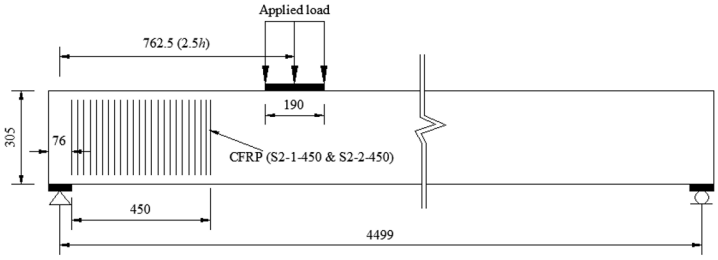

(b) Overall test rig

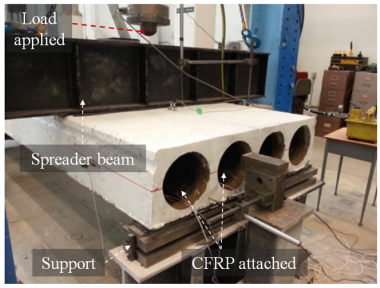

(c) Experimental setup [11]

Figure 1. Geometry and test setup of investigated slabs

2.2. Shear capacity of investigated hollow-core slabs

a. Experimental shear strength

The experimental shear strengths of the investigated HC slabs are summarized in Table 1. Among the five specimens, S2-C served as the control slab in Series 2 (i.e., without CFRP strengthening), while the remaining four specimens were strengthened with CFRP under different configurations. Specimen S2-1-450 was externally bonded with one layer of CFRP sheet measuring 450 mm in length. Specimen S2-2-450 was strengthened using two layers of CFRP, also with a bonded length of 450 mm.

Table 1. Experimental shear strength of investigated slabs

Slab ID.	Number of CFRP sheets	Length of CFRP (mm)	Exp. maximum load-carrying capacity (kN)	Shear capacity* (kN)	Failure mode
S2-C	0	0	280.5	232.9	web-shear
S2-1-450	1	450	328.0	272.4	web-shear
S2-2-450	2	450	387.0	321.4	web-shear
S2-2-450-2nd	2	450	368.0	305.6	web-shear
S2-2-450-3rd	2	450	378.0	313.9	web-shear

*Calculated from Exp. maximum load-carrying capacity, following Nguyen et al. [6].

To ensure the reliability and repeatability of the test results, the configuration of S2-2-450 was tested three times. The corresponding specimens are labeled S2-2-450, S2-2-450-2nd, and S2-2-450-3rd, as shown in Table 1. All specimens exhibited web-shear failure, and CFRP strengthening led to

a noticeable increase in both maximum load-carrying and corresponding shear capacities compared to those in the unstrengthened control slab.

b. Shear capacities according to ACI 318-19 and ACI 440.1R-15

To compare the experimental results with theoretical predictions, the shear capacities of the five tested slabs were calculated using relevant design codes [19, 20]. According to ACI 318-19 [19] the web-shear capacity of concrete members without stirrups or external strengthening can be estimated by Eq. (1), as shown below:

$$V_f = \frac{A_{fv} f_{fv} d}{s} \tag{1}$$

where A_{fv} is the total cross-sectional area of the FRP shear reinforcement within the spacing s (in mm^2), f_{fv} is the effective stress in the FRP at ultimate condition used in design, d is the effective depth of the member (in mm), and s is the center-to-center spacing of the FRP sheets along the member.

Table 2 presents a comparison between the experimental and theoretical shear capacities of HC slabs with and without CFRP strengthening. For the control specimen (S2-C), which was not strengthened with CFRP, the experimental shear capacity provided by the concrete alone was 232.9 kN. This value significantly exceeds the theoretical prediction of 83.3 kN obtained using ACI 318-19. This discrepancy reflects the known conservatism of the ACI 318-19 shear design provisions for members without transverse reinforcement, especially for HC sections with circular voids.

Table 2. Comparison of experimental and theoretical shear strengths

Slab ID.	Experimental results		Theoretical calculations	
	Experimental shear capacity due to concrete, V_c (kN)	Experimental shear capacity provided by CFRP, V_f (kN)	V_c (kN) according to ACI 318-19	V_f (kN) according to ACI 440.1R-15
S2-C	232.9	0	83.3	0
S2-1-450	232.9*	39.5	83.3	83.9
S2-2-450	232.9*	88.5	83.3	167.9
S2-2-450-2nd	232.9*	72.7	83.3	167.9
S2-2-450-3rd	232.9*	81.0	83.3	167.9

*Assumed to be equal to the shear strength of the corresponding control specimen without CFRP.

For CFRP-strengthened specimens, the additional shear contribution from CFRP (V_f) was estimated by subtracting the assumed concrete contribution (taken as equal to that of S2-C) from the total experimental capacity. The experimentally derived V_f values ranged from 39.5 kN (S2-1-450) to 88.5 kN (S2-2-450), demonstrating the clear effectiveness of CFRP in enhancing shear performance

The theoretical CFRP contributions calculated using ACI 440.1R-15 generally align with experimental trends in terms of capturing the increase in shear resistance with a greater number of CFRP layers. However, the code consistently overestimates the actual CFRP contribution to shear capacity in all tested HC slabs. This discrepancy is likely due to the code's underlying assumptions, specifically, the uniform shear stress distribution across the bonded length and full utilization of CFRP up to a predefined effective strain (typically 0.004 to 0.005) [20]. These assumptions are primarily based on conventional solid rectangular or I/T-shaped beam geometries. In contrast, HC slabs possess distinctive cross-sectional features, including longitudinal voids that reduce the effective web area and induce stress concentrations in the thin webs. Additionally, previous studies [1, 5, 21] have demonstrated that HC slabs exhibit highly non-uniform stress distributions, particularly around void

boundaries. As a result, the ACI 440.1R-15 provisions, while useful as a general design framework, lack the specificity required to accurately predict the shear behavior of CFRP-strengthened hollow-core members.

Overall, the comparison results confirm that while ACI 318-19 significantly underestimates the shear capacity of HC slabs, ACI 440.1R-15 tends to overestimate the shear contribution provided by CFRP. Therefore, in addition to theoretical calculations, alternative approaches, such as finite element analysis (FEA) should be employed to achieve more accurate predictions of the shear behavior in HC slabs strengthened with CFRP. The modeling techniques used to simulate CFRP strengthened hollow-core slabs are presented in Section 3.

3. Finite element modeling

Finite element (FE) modeling was conducted to simulate the shear behavior of HC slabs with and without CFRP strengthening. The goal of this modeling was to capture the failure mode and shear capacity observed in experiments, and to establish a validated tool for subsequent parametric studies.

3.1. Modeling techniques and material modeling

The FE models were developed using Abaqus [22], with 3D solid elements employed to represent the concrete body. Prestressing strands were modeled using truss elements embedded into the slab geometry to simulate bonded prestressing (Fig. 2). CFRP sheets were modeled using shell elements as surface layers attached to the concrete surface with a tie constraint for simplicity as debonding was not observed in the tests [10, 11, 18].

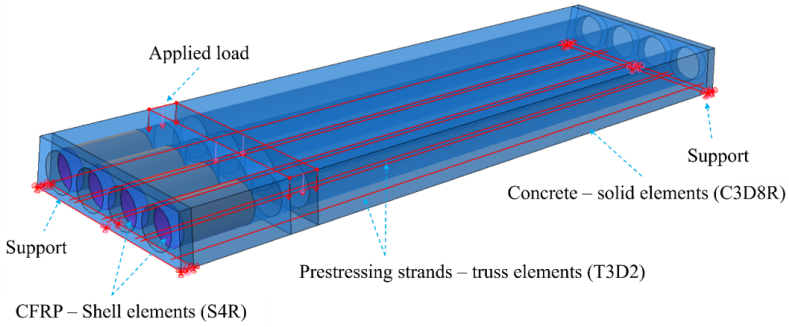

Figure 2. Modeling techniques for HC slabs with CFRP

Nonlinear material models were adopted to capture the behavior of both concrete and prestressing strand. The concrete was modeled using the Concrete Damaged Plasticity (CDP) model, incorporating tensile cracking and compressive crushing behavior [22]. CFRP was assumed to behave as a linear elastic. SikaWrap-900C, a unidirectional CFRP sheet with a thickness of 0.43 mm, was attached to the specimens using Sikadur300 Epoxy. The fiber direction of CFRP sheets was explicitly defined in the model to align with the actual vertical installation direction on the slab webs (Fig. 4). Mesh sensitivity analysis was performed to ensure numerical accuracy while maintaining computational efficiency. A mesh size of 30 × 30 mm was selected as optimal based on the convergence study, as shown in Fig. 4.

To evaluate the influence of mesh size on solution accuracy, a mesh convergence study was performed using a range of element sizes. As shown in Fig. 5, finer meshes led to only marginal improvements in the predicted peak load, while significantly increasing computational cost. A mesh size of 30 × 30 mm was found to offer a suitable balance between numerical accuracy and computational efficiency and was therefore adopted for all subsequent analyses.

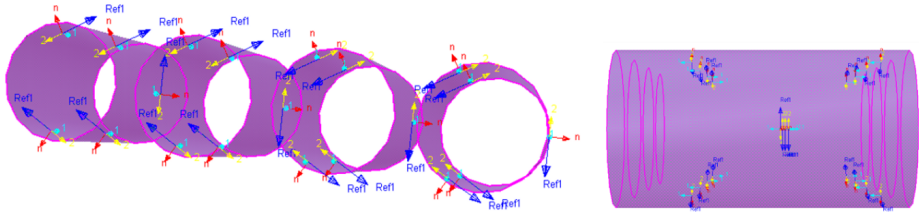

Figure 3. CFRP fiber orientation in FEM Model

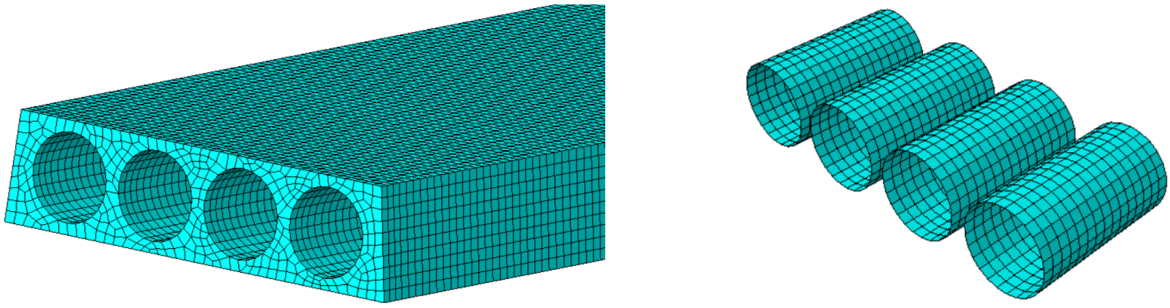

(a) Mesh discretization for concrete (b) Mesh discretization for CFRP

Figure 4. Mesh discretization of HC slabs for FEM

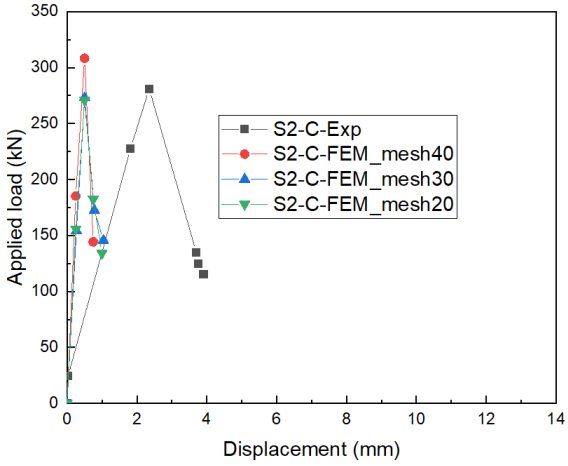

Figure 5. Mesh convergence study for FEM accuracy

3.2. Model validation

Model validation was performed by comparing the numerical results with experimental data for all the five tested slabs. Fig. 6 presents the load-displacement curves obtained from both experiments and numerical simulations while Table 3 summarizes the maximum load-carrying capacities and failure modes observed in both approaches. It is noteworthy that the displacements shown in Fig. 6 correspond to the values measured at the point of load application.

As can be seen in Fig. 6 and Table 3, the FE models closely matched the experimental shear capacities, with differences generally within 5%. The control slab (S2-C) showed a 2.6% deviation, while the CFRP-strengthened specimens exhibited variations ranging from 0.0% to 4.9%. All slabs failed in web-shear mode in both the physical tests and the simulations (Fig. 7), confirming that the models successfully reproduced the actual failure mechanism.

It should also be noted that the numerical models generally produced stiffer responses than the experimental results, particularly during the initial stages of loading. This behavior is consistent with previous studies and reflects the inherent limitations of finite element modeling in capturing existing microcracks and damage in concrete structures [1, 23]. Additionally, experimental studies have shown that HC slabs without shear reinforcement tend to fail at relatively small displacements, typically in the range of 1 mm to 3 mm [1, 6]. Given these considerations, the focus of the FE model validation was placed on peak load capacity and failure mode rather than on the accuracy of displacement predictions. Overall, the validated FE models demonstrate good agreement with experimental outcomes and provide a reliable tool for investigating the web-shear behavior of HC slabs strengthened with CFRP. Accordingly, these models are employed in the next section to conduct parametric analyses on the effects of CFRP configuration, concrete strength, prestressing level, and slab geometry on the load-carrying capacity of HC slabs.

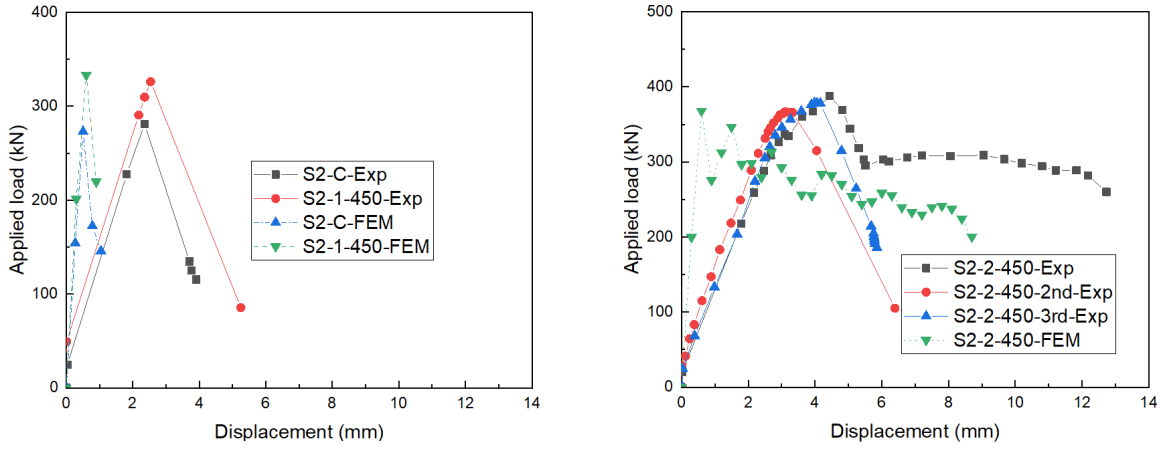

(a) Slabs S2-C and S2-1-450

(b) Slab S2-2-450 series

Figure 6. Comparison of load-displacement responses between experimental and numerical studies

Table 3. Comparison between experimental and numerical results

Slab ID.	Maximum load-carrying capacity (kN)			Failure mode	
	Experiments	FEM	Difference (%)	Experiments	FEM
S2-C	280.5	273.1	2.6	web-shear	web-shear
S2-1-450	328.0	333.3	1.6	web-shear	web-shear
S2-2-450	387.0	367.9	4.9	web-shear	web-shear
S2-2-450-2nd	368.0	367.9	0.0	web-shear	web-shear
S2-2-450-3rd	378.0	367.9	2.7	web-shear	web-shear

4. Parametric studies

Following the comprehensive validation of the FE model, a series of parametric studies was conducted to investigate the influence of key design parameters on the shear behavior of HC slabs strengthened with CFRP. The parameters examined include the CFRP configuration (length and number of layers), concrete compressive strength, prestressing level, and slab geometry and strengthening technique.

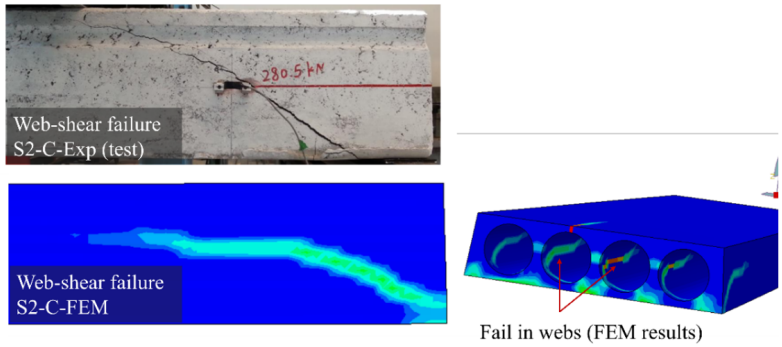

(a) Slab S2-C (without CFRP)

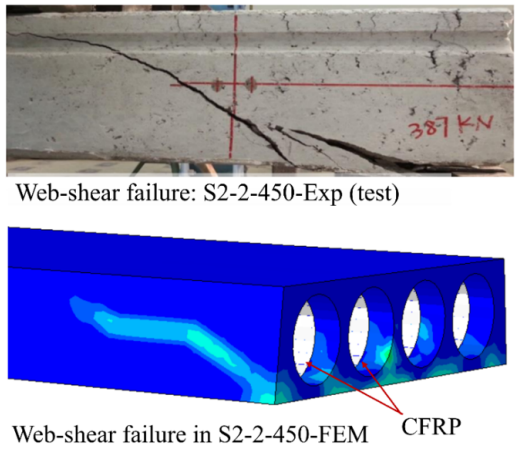

(b) Slab S2-2-450 (with CFRP strengthening)

Figure 7. Experimental and FEM failure-mode comparison

4.1. Effect of CFRP lengths and layers

To assess the impact of CFRP configuration, a range of models was analyzed by varying the bonded length (300 mm, 450 mm, and 600 mm) and the number of CFRP layers (from 1 to 4 layers). To further investigate the failure mode in slabs with increased CFRP layers, Fig. 8 presents the damage and stress distributions in S2-4-450, representing the slab strengthened with four CFRP layers and a bonded length of 450 mm, at failure. This figure provides valuable insight into the failure mechanism of CFRP-strengthened HC slabs.

As shown in Fig. 8(a), the maximum principal strain in the concrete is concentrated in the mid-web region. These localized areas exhibit strain values exceeding 3.43×10^{-2}, indicating the initiation and propagation of diagonal cracks associated with web-shear failure. Fig. 8(b) illustrates the principal strain distribution in the CFRP sheets. Although the CFRP is effectively engaged in tension, the peak strain, occurring in Layer 1 of the composite shell (the layer directly bonded to the concrete surface), reaches only 8.09×10^{-3}, remaining below the ultimate tensile strain capacity of the SikaWrap-900C material. The strain is relatively uniformly distributed along the bonded regions and around the mid-web area, where stress concentrations typically develop. Similarly, the principal stress contour in Fig. 8(c) shows that the CFRP experiences a maximum tensile stress of 121 MPa, which is significantly lower than the CFRP's ultimate tensile strength of 1120 MPa. These results clearly indicate that the failure of S2-4-450 is governed by the concrete, rather than by rupture or debond-

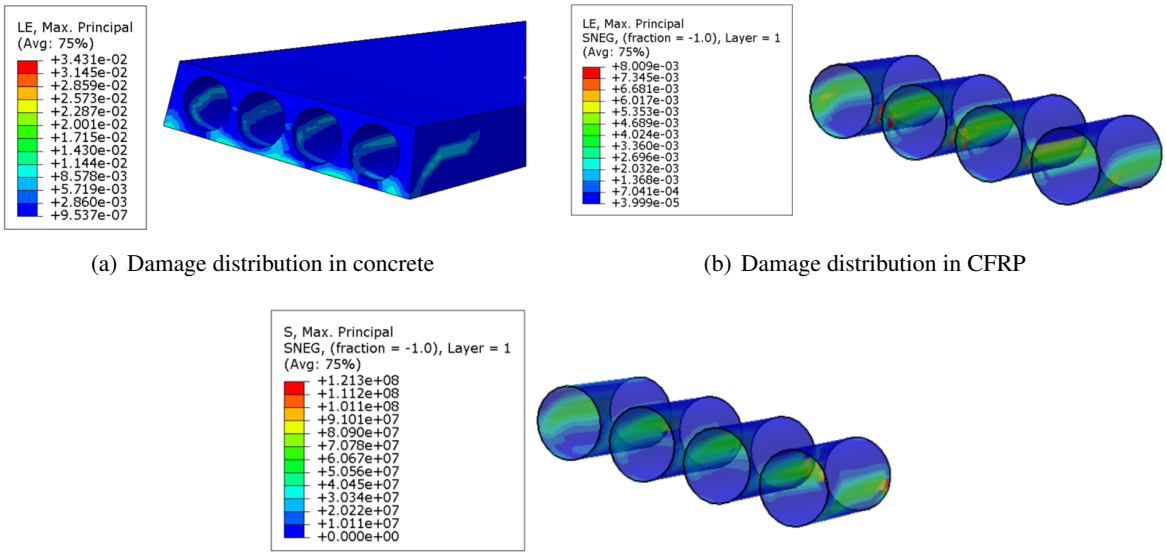

(a) Damage distribution in concrete

(b) Damage distribution in CFRP

(c) Principal stress in CFRP

Figure 8. Behavior of S2-4-450 at failure

ing of the CFRP strengthening system. Moreover, under the same loading conditions, increasing the number of CFRP layers does not alter the failure mode, as concrete failure continues to dominate the overall structural behavior.

Fig. 9 illustrates the effects of CFRP configuration, specifically, bonded length and number of layers on the shear capacity of HC slabs. It should be noted that x in Fig. 9 denotes the CFRP bonded length. It is important to note that web-shear failure was numerically observed in all investigated cases, indicating that variations in CFRP layout influenced the load-carrying capacity but did not alter the governing failure mode.

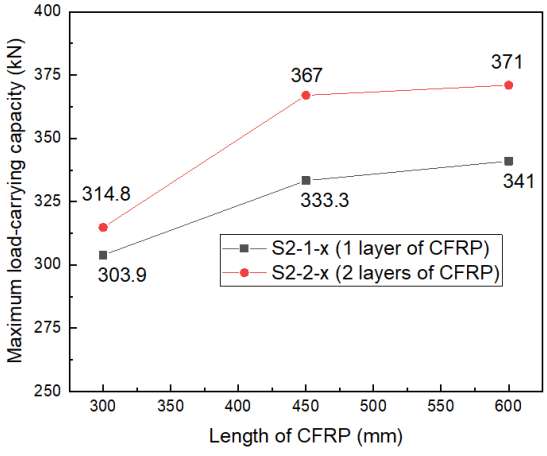

Figure 9. Effect of CFRP length on load bearing capacity of HC slabs

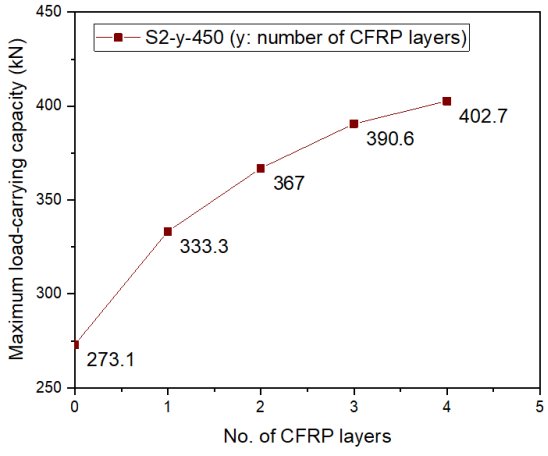

Figure 10. Effect of CFRP layers on load bearing capacity of hollow-core slabs strengthened with 450 mm length of CFRP

As can be observed from Fig. 9, increasing the bonded length of CFRP sheets from 300 mm to 600 mm results in a consistent increase in the ultimate load-carrying capacity for both single- and

double-layer configurations. For example, extending the bonded length from 300 mm to 450 mm led to a 22.0% increase in shear strength for the one-layer case (from 303.9 kN to 333.3 kN). However, further increasing the length to 600 mm provided a marginal additional gain of only 2.3% (from 333.3 kN to 341.0 kN). This diminishing return suggests that beyond a certain effective anchorage length, additional CFRP does not proportionally contribute to shear resistance due to bond limitations or ineffective stress transfer in the extended region.

Fig. 10 highlights the influence of the number of CFRP layers while maintaining a fixed bonded length of 450 mm. The shear capacity increases significantly with each additional layer up to three layers, beyond which the improvement rate becomes less pronounced. For instance, increasing the number of layers from one to two improved the peak load from 333.3 kN to 367.0 kN (a 10.1% increase), and from two to three layers yielded an additional 6.4% gain. However, adding a fourth layer only raised the capacity by 3.1% compared to the three-layer configuration.

From a structural and economic standpoint, the most efficient or optimal configuration is achieved with two to three CFRP layers at a CFRP length of 450 mm. This setup provides substantial improvement in shear resistance (over 34% compared to the unstrengthened specimen) while avoiding excessive material use and diminishing structural returns observed with longer lengths or higher layer counts. This balance between performance gain and material efficiency makes the configuration suitable for practical strengthening applications of HC slabs.

4.2. Effect of concrete compressive strength

The influence of concrete compressive strength on shear capacity was examined for three classes: 50 MPa, 60 MPa, and 70 MPa. It should be noted that the compressive strengths refer to cylinder strengths measured using 150 × 300 mm specimens. As shown in Table 4 and Fig. 11, higher concrete strength led to increased load-carrying capacity across all slab types.

Table 4. Maximum load-carrying capacity with different concrete strengths

Slab ID.	f_c' = 50 MPa	f_c' = 60 MPa	f_c' = 70 MPa
S2-C-FEM	219.8	273.1	309.4
S2-1-450-FEM	263.8	333.3	371.0
S2-2-450-FEM	306.2	367.9	404.3

For the control slab (S2-C-FEM), increasing the concrete compressive strength from 50 MPa to 70 MPa resulted in a rise in peak load from 219.8 kN to 309.4 kN. A similar trend was observed for the CFRP-strengthened slab (S2-2-450-FEM), where the peak load increased from 306.2 kN to 404.3 kN over the same strength range. These results are consistent with the analysis presented in Section 4.1, which showed that, although the CFRP contributes to stress redistribution and crack control, the concrete substrate ultimately governs the failure due to its brittle response under shear loading. This underscores the importance of enhancing the shear capacity of the concrete itself, even when external strengthening systems are employed. Furthermore, the observed improvement in load capacity with higher concrete strength reflects a synergistic effect between the upgraded concrete and the CFRP reinforcement. Strengthening the intrinsic properties of the concrete not only delays the onset of failure but also maximizes the effectiveness of the external CFRP system in resisting web-shear failure.

4.3. Effect of prestressing level

To evaluate the influence of prestressing force on shear capacity, numerical models were developed with three different effective prestress levels: 1020 MPa (baseline), 110% (1122 MPa), and

120% (1224 MPa). These values account for an assumed 18% loss due to common prestressing effects, including elastic shortening, creep, shrinkage, and relaxation. As illustrated in Fig. 12, increasing the prestress level led to a reduction in shear capacity. Specifically, the peak load of specimen S2-1-450 decreased from 333.3 kN at the baseline level to 321.2 kN (−3.6%) at 110% and further dropped to 292.0 kN (−12.4%) at 120% prestress.

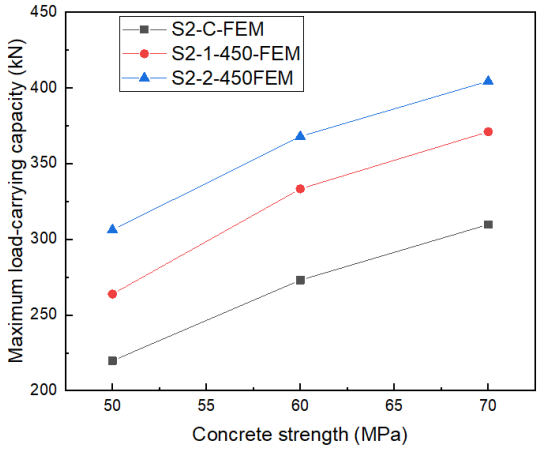

Figure 11. Effect of concrete strength on load-carrying capacity of HC slabs with and without CFRP

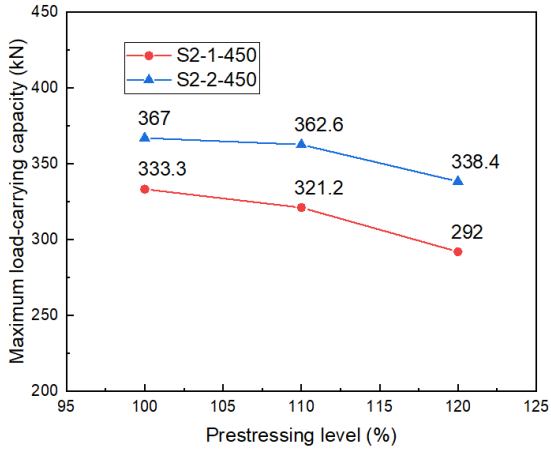

Figure 12. Effect of prestressing level on load bearing capacity of HC slabs with CFRP

This counterintuitive trend is consistent with previous experimental findings for unstrengthened HC slabs [3, 10, 24] and may be attributed to additional shear stresses that develop in the concrete web, particularly within the transmission length region as discussed in prior studies [1, 21]. The findings suggest that increasing the prestressing level does not necessarily improve the shear resistance of HC slabs, whether or not they are strengthened with CFRP.

4.4. Effect of slab geometries and strengthening techniques

To examine the impact of slab geometry on shear behavior, additional finite element models were developed for HC slabs with a height of 400 mm and non-circular voids (denoted as HC.400). This slab geometry, shown in Fig. 13, was selected based on prior experimental studies [1, 6] but had not been numerically investigated in the context of CFRP strengthening.

As presented in Table 5, the base slab HC.400, without CFRP, exhibited a peak load of 351.4 kN. To evaluate strengthening efficiency, two different CFRP application schemes were modeled: (i) full-height strengthening of the entire side web (HC.400-1-450, HC.400-2-450, HC.400-3-450), and (ii) web-only strengthening limited to the voided area (HC.400-1-450-a). All slabs used a CFRP bonded length of 450 mm, with the number of layers ranging from one to three. The strengthening layouts are illustrated in Fig. 14.

As shown in Table 5, full-height CFRP strengthening significantly enhanced the shear capacity. A single CFRP layer (HC.400-1-450) increased the peak load to 527.3 kN (50.1% improvement), while three layers (HC.400-3-450) pushed it to 568.9 kN (61.9% improvement). In contrast, the web-only strengthening scheme (HC.400-1-450-a) yielded a peak load of 433.9 kN, corresponding to a 23.5% gain, notably lower than the full-height configuration with the same number of CFRP layers.

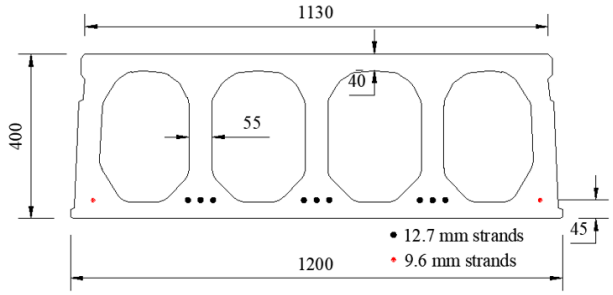

(a) Cross section of HC slabs with 400 mm height

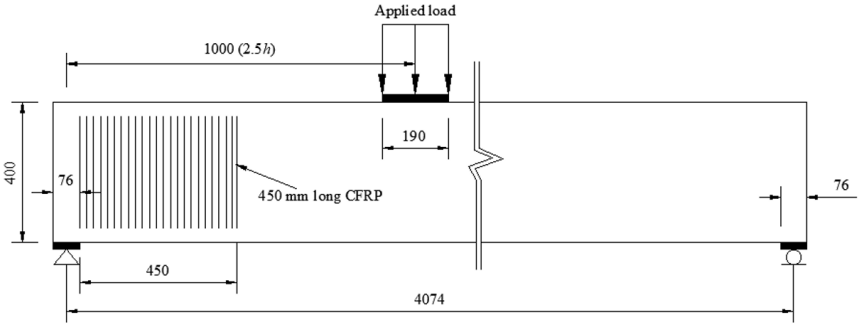

(b) Applied loading configuration

Figure 13. Details of Slab HC.400 (non-circular void slab)

Table 5. Shear capacity of 400 mm HC slabs with different CFRP strengthening techniques

Slab ID.	Strengthening technique	Maximum load-carrying capacity (kN)	% improvement
HC.400	whole core	351.4	0
HC.400-1-450	whole core	527.3	50.1
HC.400-2-450	whole core	557.2	58.6
HC.400-3-450	whole core	568.9	61.9
HC.400-1-450-a	web area	433.9	23.5

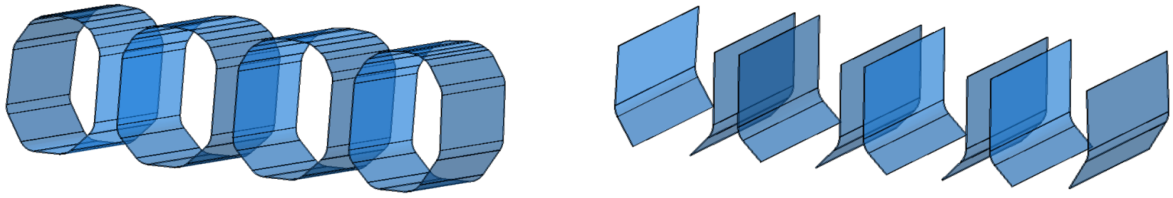

(a) CFRP layout in HC.400-1-450

(b) CFRP layout in HC.400-1-450-a

Figure 14. Strengthening techniques for the 400 mm slab

Fig. 15 presents the load-displacement responses, which confirm the superior performance of the full-height strengthening approach in terms of both load capacity and stiffness. All models failed in web-shear mode, as illustrated in Fig. 16, indicating that while CFRP delayed failure and increased capacity, it did not fundamentally alter the failure mechanism.

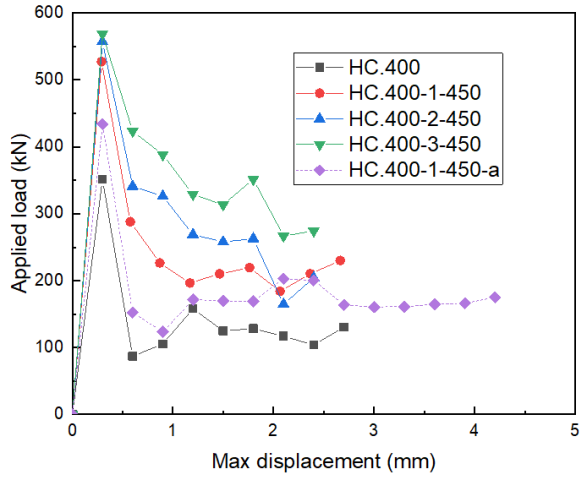

Figure 15. Load-displacement curves of HC.400 series

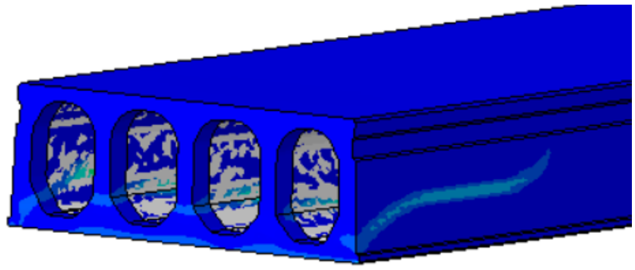

Figure 16. Typical web-shear failure in HC.400-2-450 Slab

Fig. 17 compares the effectiveness of CFRP strengthening across two slab series: the S2 series (S2-1-450, S2-2-450, S2-3-450) with 305 mm deep slabs with circular voids, and the HC.400 series (HC.400-1-450, HC.400-2-450, HC.400-3-450) with 400 mm deep slabs with non-circular voids. Each series includes slabs strengthened with one, two, and three layers of CFRP with a bonded length of 450 mm.

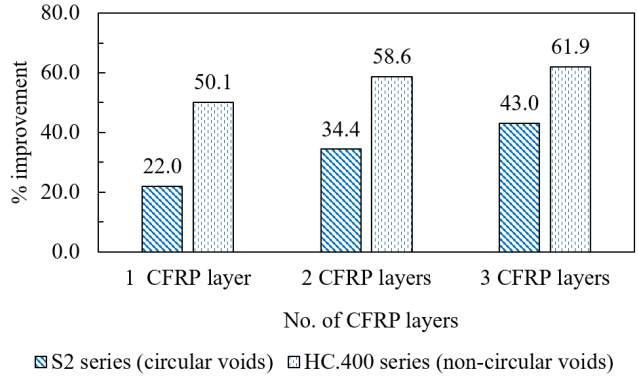

Figure 17. Comparison of CFRP strengthening effectiveness between S2 and HC.400 Slab series

Fig. 17 clearly shows that the HC.400 series achieved higher absolute and relative improvements in shear capacity compared to the S2 series for the same CFRP configurations. For instance, with two CFRP layers, HC.400-2-450 reached a peak load of 557.2 kN, representing a 58.6% increase over the unstrengthened HC.400 slab, while S2-2-450 achieved a peak load of 367.0 kN, 34.4% higher than

the S2-C control slab. This trend is consistent across all three configurations and suggests that CFRP strengthening is more effective in deeper slabs with non-circular voids. This enhanced effectiveness may be attributed to the following factors: (1) the increased web area in deeper slabs allows for greater CFRP bonding and improved load transfer, and (2) the higher initial shear capacity of the HC.400 slab amplifies the relative contribution of CFRP strengthening.

In summary, the numerical investigation highlights the important role of slab geometry in influencing the efficiency of CFRP strengthening. The findings suggest that CFRP may be more effective in HC slabs with non-circular voids and greater depth, provided that adequate bonding and appropriate strengthening layouts are ensured. However, further research is recommended to investigate this phenomenon in a more comprehensive and systematic manner.

5. Conclusions

This study conducted a comprehensive numerical investigation into the web-shear behavior of HC slabs strengthened with externally bonded CFRP sheets. FE models were developed and validated against experimental data to capture load capacity, failure modes, and response characteristics. The key findings are summarized as follows:

- Comparison with theoretical predictions revealed notable discrepancies: ACI 318-19 significantly underestimated the shear capacity of unstrengthened HC slabs, while ACI 440.1R-15 consistently overestimated the CFRP contribution in strengthened HC slabs.

- The validated FE models reasonably reproduced the experimental shear capacities and failure modes for both strengthened and unstrengthened slabs, with deviations within 5%, confirming their suitability for extended parametric studies.

- CFRP strengthening significantly improved web-shear resistance. Increasing the bonded length and number of CFRP layers enhanced peak load capacity, though gains diminished beyond two to three layers or lengths exceeding 450 mm. An optimal configuration was identified as two to three CFRP layers with a 450 mm bonded length.

- Higher concrete compressive strength led to substantial improvements in shear capacity. A clear synergistic effect between concrete strength and CFRP was observed, emphasizing the role of base material quality in strengthening performance.

- Increasing effective prestress levels reduced shear capacity, consistent with prior findings for unstrengthened HC slabs. This trend is attributed to additional internal shear stresses in the transmission region, indicating that higher prestress does not necessarily enhance shear resistance for HC slabs strengthened with CFRP.

- Slab geometry significantly influenced strengthening efficiency. Deeper slabs with non-circular voids (e.g., HC.400 series) achieved greater performance gains from CFRP applications than shallower slabs with circular voids. Full-height CFRP web strengthening proved more effective than localized application, highlighting the importance of tailored design strategies.

Acknowledgement

This research is funded by Vietnam National Foundation for Science and Technology Development (NAFOSTED) under grant number 107.01-2021.65.

References

[1] Nguyen, T. H., Tan, K.-H., Kanda, T. (2019). Investigations on web-shear behavior of deep precast, prestressed concrete hollow core slabs. *Engineering Structures*, 183:579–593.

[2] Shakya, A., Kodur, V. (2015). Response of precast prestressed concrete hollowcore slabs under fire conditions. *Engineering Structures*, 87:126–138.

[3] Pajari, M. (2005). *Resistance of prestressed hollow core slabs against web shear failure*. Technical Research Centre of Finland.

[4] Pajari, M. (2009). Web shear failure in prestressed hollow core slabs. *Journal of Structural Engineering*, 42(4):83–104.

[5] Nguyen, H. T. N. (2020). Shear behavior of deep precast/prestressed concrete hollow-core slabs with and without fibers at ambient and under fire conditions. PhD thesis, Nanyang Technological University.

[6] Nguyen, H. T., Tan, K. H., Kanda, T. (2020). Effect of polypropylene and steel fibers on web-shear resistance of deep concrete hollow-core slabs. *Engineering Structures*, 210:110273.

[7] Fan, S., Nguyen, T. H., Ren, H., Wang, P. (2024). Data-driven shear strength predictions of prestressed concrete hollow-core slabs. *Journal of Building Engineering*, 95:110343.

[8] Hawkins, N. M., Ghosh, S. (2006). Shear strength of hollow-core slabs. *PCI Journal*, 51(1):110–114.

[9] Walraven, J. C., Mercx, W. P. M. (1983). The bearing capacity of prestressed hollow core slabs. *Heron*, 28(3).

[10] Meng, X., Cheng, S., Ragaby, A. J. P. J. E. (2019). Shear strengthening of prestressed concrete hollow-core slabs using externally bonded carbon-fiber-reinforced polymer sheets. *PCI Journal*, 64(5).

[11] Meng, X., Cheng, S., Ragaby, A. J. R. L. E. (2016). Experimental study on a novel shear strengthening technique for precast prestressed hollow-core slabs. In *Resilient Infrastructure*.

[12] Sakbana, A., Mashreib, M. (2020). Finite element analysis of CFRP-reinforced concrete beams. *Revista Ingeniería de Construcción*, 35(2):148–169.

[13] Elgabbas, F., El-Ghandour, A. A., Abdelrahman, A. A., El-Dieb, A. S. (2010). Different CFRP strengthening techniques for prestressed hollow core concrete slabs: Experimental study and analytical investigation. *Composite Structures*, 92(2):401–411.

[14] Nhung, P. T., Nhan, D. X., Vu, N. K. A., Tung, T. N. T., Tung, N. X., Tan, N. N., Hieu, D. D. (2023). Investigation of parameters affecting the load-carrying capacity of concrete beams without stirrups strengthened in shear with CFRP sheets. *Journal of Science and Technology in Civil Engineering (JSTCE) - HUCE*, 17(3V):17–34. (in Vietnamese).

[15] Tran, A.-D., Du, D. H., Vu, C. H., Nguyen, H. G., Nguyen, N. T. (2025). Influence of Rectangular Opening Layout in GFRP-Reinforced Concrete One-Way Slabs Strengthened with CFRP Sheets. In *Proceedings of the 3rd Vietnam Symposium on Advances in Offshore Engineering*, volume 590, Springer Nature Singapore, 249–258.

[16] Nguyen, N. D., Lam, D. T., Tan, N. N. (2023). Flexural-shear strengthening of reinforced concrete T-beams subjected to asymmetric loading using CFRP system combined by NSM strips and U-wraps. *Journal of Science and Technology in Civil Engineering (STCE) - HUCE*, 17(4):48–65.

[17] Nguyen, D. N., Dang, T. L., Nguyen, N. T. (2025). Numerical investigation of T-Beam reinforced concrete strengthened in flexure and shear Using CFRP. *Journal of Science and Technology in Civil Engineering (JSTCE) - HUCE*, 19(1V):94–108. (in Vietnamese).

[18] Wu, Y. (2015). Shear strengthening of single web prestressed hollow core slabs using externally bonded FRP sheets. Master's thesis, University of Windsor.

[19] ACI 318-19 and ACI 318RM-19 (2019). *Building code requirements for structural concrete (ACI 318-19) and commentary (ACI 318RM-19)*. American Concrete Institute, Farmington Hills, MI.

[20] ACI 440.1R-15 (2015). *Building Code Requirements for Structural Concrete Reinforced with Glass Fiber-Reinforced Polymer (GFRP) Bars - Code and Commentary*. American Concrete Institute, Farmington Hills, MI.

[21] Yang, L. (1994). Design of prestressed hollow core slabs with reference to web shear failure. *Journal of Structural Engineering*, 120(9):2675–2696.

[22] Simulia, A. V. (2017). *Documentation*. Dassault Systems.

[23] Demir, A., Ozturk, H., Dok, G. (2016). 3D Numerical Modeling of RC Deep Beam Behavior by Nonlinear Finite Element Analysis. *Disaster Science and Engineering*, 2(1):13–18.

[24] Sozen, M. A. (1957). Strength in shear of prestressed concrete beams without web reinforcement. PhD thesis, University of Illinois at Urbana-Champaign.